Experimental and Numerical Investigation into the Adhesion of PVD Coatings on Minting Dies

Jason Tunis[1], Xin Wang[1,*] and Xianyao Li[2]

[1] Department of Mechanical and Aerospace Engineering, Carleton University,
Ottawa, Ontario, K1S 5B6, Canada
[2] Corporate Engineering, Royal Canadian Mint, 320 Sussex Drive,
Ottawa, Ontario, K1A 0G8, Canada
*Corresponding author: xwang@mae.carleton.ca

Abstract This paper reports on the adhesion characterization of a PVD coating deposited onto mirror polished and laser frosted minting die surfaces. Experimental and numerical methods are both used to study the adhesion of the PVD coating. Stepped Rockwell-C indentation testing method is used to experimentally examine the coating adhesion. Finite element analyses of the stepped indentation adhesion tests are performed using critical loads determined from experimental testing. The analyses are performed to determine the stresses produced at the coating-substrate interface prior to coating adhesion failure and characterize the coating adhesion. The indentation simulations found that large compressive, shearing, and opening stresses were present at the coating-substrate interface in the regions where coating delamination was observed during experimental testing. The value of the compressive, opening, and shear critical stresses are found during finite element simulation of the indentation. These stress components provide good quantification of the coating adhesion strength.

Keywords PVD coating, adhesion, indentation tests, critical stresses

1. Introduction

Advances in the minting of coinage have led to the use of highly specialized die coatings. These coatings, in the form of thin hard films, are applied to die surfaces to improve their surface performance and increase their service life. The Royal Canadian Mint (RCM) uses a Cr-Ti-N based physical vapour deposition (PVD) coating applied to a hardened tool steel using magnetron sputter ion plating [1].

Coin forming is achieved by the striking of a blank disc between two dies. A collar surrounding the blanks circumference limits radial expansion of the blank during striking. The forming process produces large stresses in the die coating and steel substrate. The coating is expected to survive thousands to multiple hundreds of thousands of these impacts. To achieve long die life, the coating must be well adhered to the tool steel substrate and for this reason it is very important to ensure that adequate adhesion is achieved.

In recent years, laser engraving and frosting has started to be used on minting dies prior to coating to produce highly detailed coins with new surface finishes. Limited research has been completed in examining the effect of these new surface finishes on coating adhesion.

Many test methods exist for examining the adhesion between the coating and substrate. Among them are the indentation and the scratch adhesion tests, both of which are commonly used for testing the adhesion of thin hard coatings. These adhesion tests can be used to characterize the coating adhesion semi-quantitatively and with added analyses quantitatively [2].

Recently, the combination of experimental testing and numerical simulation has been used by several researchers to quantify coating adhesion. Indentation adhesion tests have been used together with finite element simulations to quantify the adhesion of thin hard coatings, see Pachler et al. [3], Nygards et al. [4], Xu et al. [5] and Sun et al. [6], for examples.

In this paper, the combination of experimental testing and finite element simulations of indentation tests is used to quantify the adhesion of the PVD coating used by the RCM. The adhesion to a mirror polished surface and to several laser frosted surfaces are examined. The critical loads determined during experimental testing are used in the finite element simulations. The maximum opening stress, maximum shear stress and maximum compressive stress values at the coating-substrate interface determined from finite element simulations are used to characterize the adhesion strength.

2. Background

In this section, an examination of the adhesion of thin-film systems and the testing of their adhesion are summarized. A detailed review of the use of experimental adhesion testing combined with numerical simulations to quantify the stresses produced during testing is presented for the indentation tests.

2.1. Adhesion of Thin-Film Systems

Depositing a thin hard film onto a softer substrate is only beneficial if the film has good adhesion and does not fail during normal operation. For this reason, coating adhesion must be closely examined and well understood.

Adhesion is defined as an attractive process between dissimilar materials which brings two compounds into direct contact. The strength of adhesion is difficult to quantify, but can be determined qualitatively, semi-quantitatively, and under certain scenarios quantitatively using various adhesion tests. The adhesion measurement between two materials estimated during experimental testing is generally dependent on the test method employed to determine it. For this reason, adhesion test results must be stated with the method used to determine them. Common adhesion test methods are the indentation test, scratch test, peel test, tape test, blister test, self loading test, beam bending test, pull test, and laser spallation test [2]. The indentation adhesion tests are reviewed below. Indentation adhesion tests will be used in this paper to quantify the adhesion strength of the PVD coating.

2.2. Indentation Adhesion Test

Indentation testing was first developed to quantify the hardness of materials. By applying a specific load using a standardized indenter, the hardness of a material can be determined by measuring the size of the resultant indentation crater and/or the vertical displacement of the indenter. Several varieties exist and the following is a list of the most common indentation tests: Brinell hardness test, Rockwell hardness test, Vickers hardness test, and Knoop hardness test. Corresponding ASTM standards can be found for these various tests.

Indentation tests can also be used to test the adhesion of coatings. The procedure is very similar to indentation tests completed to determine hardness except instead of measuring the indentation size, the damage caused to the coating is examined. A schematic of an indentation adhesion test is shown in Figure 1 and the apparatus used for testing in this paper is shown in Figure 2. The advantages of this test method are:

- sample preparation is minimal
- the test equipment is readily available (cost effective)
- test standards are well established
- semi-quantitative or quantitative results can be achieved

2.3. Finite Element Simulation of Indentation Adhesion Testing

In order to further understand the causes of coating failures during indentation adhesion testing, the stress state in the coating can be determined using finite element analysis. Radial and circular cracking the coatings has been studied by examining the tangential and radial stresses induced during indentation. This provides insight into through thickness coating failure. Delamination along the coating-substrate interface (adhesion failure) has been studied by examining the shear and opening stresses at the interface. Compressive stress in the coating are also be studied if buckling failure of the coating is present in experimental testing.

In this paper, indentation adhesion tests will be performed to obtain the critical load at which adhesion failure occurs for the PVD coating on each die surface. These loads will then be used in finite element analysis. The corresponding maximum opening, shear, and compressive stresses at the coating-substrate interface will be used to quantify the coating adhesion.

3. Experimental Testing of Coating Adhesion

The experimental setup, procedure, and results of the adhesion testing completed on the hard PVD coating used by the RCM are presented in this section. Eight dies were prepared and the adhesion of the coating to a mirror surface and to four laser frosted surfaces was investigated using a stepped variation of the Rockwell-C indentation adhesion test.

3.1. Sample Preparation

The dies used for testing were machined from a soft annealed bar stock of a tool steel. The bar stock was first cut to length and the top and bottom surface were machined flat using a lathe. The machined substrates were then heat treated using a vacuum heat treatment furnace. The top surface of the substrates was then polished to a mirror surface. In total eight test dies were manufactured. Four of the eight dies were laser frosted on three quarters of their surface, each with a different surface frosting (termed as Bullion, Glass Bead, Four-to-One, and Aluminum Oxide, respectively) as shown in Figure 3. The remaining four were not laser frosted. After preparing the die surface, the hard PVD coating was applied using a Teer UDP650/4 magnetron sputter ion plating system. The thickness of the Cr-Ti-N PVD coating is controlled to between two and three μm.

3.2. Stepped Indentation Adhesion Test

The stepped indentation adhesion test is a variation on the Rockwell-C indentation adhesion test. The indentation load is increased in steps and the produced indentation craters are examined for signs of coating failure. Coating delamination was defined as the failure criteria and the highest loading case which causes no coating delamination was examined for each coated die surface. The maximum survivable load provides a semi-quantitative measurement of the PVD coating adhesion and will also be used later in section 4 during finite element simulations. The maximum survivable load will be the indentation load used in simulations of indentation tests examining the stress state at the coating-substrate interface prior to coating adhesion failure.

The experimental apparatus is the same as that used for the Rockwell-C indentation adhesion tests, but for this test multiple loading conditions were used. The available weight options were 15, 30, 45, 60, 100, 150 kg_f and all were used.

3.3 Experimental Results

Multiple indentation tests were performed on each different die surface to determine the maximum load each respective coating-substrate systems could withstand. More tests were performed at loadings where the coating changed from a pass to a fail. The stepped indentation tests for the PVD coating on the mirror surface and laser frosted surfaces are conducted, in this manner. The following subsections provide observations for each die surface.

PVD coating deposited on a mirror surface

A summary of the results for the stepped indentation test of the PVD coating deposited on a mirror surface is shown in Figure 4. The indentation tests using a 45 kg_f load caused a delamination for half of the 14 tests and the tests performed using a 30 kg_f load only caused one delamination out of 14 tests. The typical results for indentations of 30 kg_f can be seen in Figure 5. Cracking is visible around the circumference of the indent crater and small radial cracks are also visible. The typical results of indents using 60, 100, and 150 kg_f were also obtained. Small delaminations are visible around the edge of the craters and the cracking is no longer radial. The 30 kg_f load was found to be the maximum load the coating could reliably survive without coating delamination.

PVD coating deposited on a Bullion type laser frosted surface

The Bullion test results show that the coating failed all three 45 kg_f and passed all three 30 kg_f. Figure 6 shows typical results for 30 kg_f loading conditions. For loads at 30 kg_f loading condition only causes cracking, while the higher loading condition causes cracking and delamination. Therefore, the 30 kg_f loading was found to be the maximum survivable indentation load for the Bullion laser frosted surface.

PVD coating deposited on a Glass Bead type laser frosted surface

The Glass Bead test results show that the maximum safe load is 15 kg_f. Typical results are shown in Figure 7 for 15 kg_f loading conditions. The 15 kg_f loading condition only causes cracking, while the 30 kg_f loading condition causes cracking and delamination. The 15 kg_f loading case was found to be the maximum survivable load for the Glass Bead laser frosted surface.

Note the other two types of laser frosted surfaces (four-to-one, and aluminum oxide), the surface roughness makes the finding of coating failure difficulty, therefore, from now on, only Bullion and Glass Bead laser surfaces are further studied together with mirror finished surface.

4. Finite Element Simulation of Indentation Adhesion Testing

This section presents the two-dimensional axisymmetric finite element simulation of indentation adhesion tests using ABAQUS [7]. The simulations are used to determine the stress state at the coating-substrate interface prior to coating failure. Focus is placed on the opening stress, the shear stress, and compressive stress at the interface since these stress components are the likely cause of delamination growth. The maximum survivable indentation loads estimated using the stepped indentation adhesion tests in Section 3 are used as indentation loads in the simulations. Simulations are completed using 15 and 30 kg_f indentation loads. The 15 kg_f simulation represents the PVD coating deposited on the Glass Bead laser frosted surface and the 30 kg_f represents the PVD coating deposited on the mirror surface and Bullion laser frosted surface.

The finite element model geometry, boundary conditions, material properties, and mesh design will be outlined below, followed by a presentation of the computed stress state at the coating-substrate interface. The opening, shear, and compressive stresses at the coating-substrate interface will provide a quantification of the PVD coating adhesion strength to the mirror surface and Glass Bead and Bullion laser frosted surfaces.

4.1 FEM Model Setup, Geometry, and Boundary Conditions

The indentation adhesion test is axisymmetric and therefore a simplified axisymmetric finite element model was used to simulate the test. ABAQUS/Standard version 6.8 [7] was used for the finite element analysis. The indentation adhesion test consists of three steps, first the indenter is lowered to the die surface and then load is applied and ramped up to the maximum load. Finally the load is removed and the indenter is raised off the die surface. The indentation test was modeled as quasi-static and all time-dependant effects were neglected. The indenter and die geometry and the boundary conditions are presented below.

Indenter Geometry

The indenter geometry used is that of a Rockwell-C cone indenter as defined by ASTM E18-8b [8]. The indenter has a 200 μm radius cone tip and 60° half angle. The axisymmetric indenter model was defined as presented in Figure 8 and the geometry was fixed to a reference point. Displacements and loads are applied to the indenter by moving or loading the reference point.

Die Geometry

The die geometry used is shown in Figure 9. An axisymmetric boundary condition is placed on the axis of symmetry and vertical displacement is fixed at the bottom of the model. The PVD coating thickness used by the RCM is controlled to be between two and three microns. The average of the thickness range, 2.5 μm, was selected for the model. The overall size of the die segment modeled was one millimetre by one millimetre and was selected after testing different model sizes. Multiple model sizes were tested and the model size selected was chosen since it minimized the model size while not affecting the stress values at the coating-substrate interface.

4.2 Material and Interface Properties

Indenter Properties

The Rockwell-C indenter tip is made of diamond which is significantly harder than the die substrate. The deflection of the diamond indenter during loading up to the maximum indentation load used, 30 kg_f, is negligible and therefore it was modeled as an analytical rigid body.

Substrate Properties

The substrate of the die samples used for experimental testing was a tool steel and it was modeled as an elastoplastic material with isotropic strain hardening. The material properties used during indentation simulations are shown in Table 1. The elastic modulus and yield strength values were taken from a tool steel material datasheet [9]. The Ramberg-Osgood stress strain relationship was used to define the materials strain hardening as follows:

$$\varepsilon = \frac{\sigma}{E} + \alpha \frac{\sigma_y}{E} \left(\frac{\sigma}{\sigma_y} \right)^n \quad (1)$$

where α is the yield offset and n is the strain hardening exponent. Assuming an industry standard strain value of 0.2 % was used when defining the yield strength of the tool steel, α can be calculated to be 0.18.

The strain hardening exponent was determined using a numerical and experimental approach as described by J. Yan et al. [10]. A strain hardening exponent value (n) of 15 was found to agree well with the experimental data and therefore n = 15 was used as the strain hardening exponent for the substrate.

Coating Properties

The material properties used for defining the Cr-Ti-N based hard PVD coating are shown on Table 2. The elastic modulus, yield strength, and Poisson's ratio values for the PVD coating were determined using nano-indentation testing completed by McLean [11]. As recommended by Piana et. al [12], Ramberg-Osgood strain hardening parameters of α = 1 and n = 100 were chosen to produce a material with minimal strain hardening.

Interface Properties

The loading conditions used during the indentation test simulations are below the failure load of the coating-substrate interface, therefore the interface between the coating and substrate was modeled as being in perfect adhesion.

The interaction between the indenter and the coating surface was defined using the "Interaction Module" built into ABAQUS [7]. A contact pair was defined, with indenter being the master surface and the coating surface being the slave surface. The indenter is ideal for the master surface because it is an analytical rigid body and is accurately defined without discretization using an arc and a line. To complete the interaction definition the tangential and normal behaviour between the two surfaces must be defined. The tangential behaviour was defined as frictionless as recommended by Piana et al. [12]. Neglecting friction has an insignificant effect on the results of indentation test simulations [12]. The normal behaviour was defined as "hard contact", which does not allow the coating top surface nodes to pass through the indenter geometry. Separation after contact was permitted to allow for unloading of the indenter.

4.3 Mesh Design

The mesh was refined towards the indentation location to properly model the large deformation and steep stress gradient. Due to the large deformation in the region of the indentation, it is important to enable nonlinear geometry in ABAQUS [7]. The finite element models were discretized using 4-node bilinear axisymmetric quadrilateral elements, which are defined as CAX4R in the ABAQUS element library [7]. This element type is a first order continuum element and uses reduced integration. Reduced integration lowers the number of constraints introduced by the elements, thus decreasing the CPU time and storage requirements and also preventing volumetric locking. The "hourglass control" is enabled to address the potential zero energy deformation modes (hourglass modes) introduced when using reduced integration [7]. The mesh design of the

coating-substrate system is shown in Figure 10. The shown model uses 4 element layers to discretize the coating, 8, 16 and 25 layered meshes were also used for mesh refinement analysis. A node set is defined along the coating-substrate interface for easy retrieval of displacement and stress data during post processing.

4.4. FEA results

Stress Transformation

In order to properly evaluate the stresses at the coating-substrate interface, the global stress components obtained from ABAQUS [7] must be transformed into local coordinate stress components. Figure 11 shows how the global coordinates axes (x-y-z) relate to the local coordinates axes (x'-y'-z'). The x' local coordinate axis is parallel to the coating-substrate interface and the y' local coordinate axis is perpendicular to the coating-substrate interface. The following equations show how the global stress components were transformed into local stress components [13]:

$$\sigma_{x'x'} = \frac{\sigma_{xx}+\sigma_{yy}}{2} + \frac{\sigma_{xx}-\sigma_{yy}}{2}\cos 2\theta + \tau_{xy}\sin 2\theta \quad (2)$$

$$\sigma_{y'y'} = \frac{\sigma_{xx}+\sigma_{yy}}{2} - \frac{\sigma_{xx}-\sigma_{yy}}{2}\cos 2\theta - \tau_{xy}\sin 2\theta \quad (3)$$

$$\sigma_{z'z'} = \sigma_{zz} \quad (4)$$

$$\tau_{x'y'} = \frac{\sigma_{xx}-\sigma_{yy}}{2}\sin 2\theta + \tau_{xy}\cos 2\theta \quad (5)$$

Going forward, $\sigma_{x'x'}$, $\sigma_{y'y'}$, $\sigma_{z'z'}$, and $\tau_{x'y'}$ will be called the radial stress, the opening stress, the hoop stress and the shear stress. Note that the stress component ($\sigma_{x'x'}$) named radial stress is not perfectly radial once x' is not aligned with x, but the name is still used for simplicity. The two out of plane shear stress components, τ_{xz} and τ_{yz}, are zero due to the problem being axisymmetric.

Results

The stress state at the coating-substrate interface was examined at two times during the simulations, first when the maximum indentation load is applied and second after unloading of the indenter. Von Mises stress, radial stress ($\sigma_{x'x'}$), hoop stress ($\sigma_{z'z'}$), opening stress ($\sigma_{y'y'}$), and shear stress ($\tau_{x'y'}$) along the coating-substrate interface for both the maximum load and after unloading states are obtained. The stress in the coating material and substrate material at the interface are both included in the presented stress results.

Von Mises Stress Results

Von Mises stress contour plots are shown in Figure 12 (maximum load case) and Figure 13 (after unloading) for the 30 kg_f indentation case. At maximum load, large von Mises stresses occur in the coating under the indenter and extend outward past the indentation radius. After unloading, the von Mises stress is significantly reduced inside the crater region, but large values are still present outside the indentation radius. Very low von Mises stress gradients are present near the bottom and right edges of the model, which shows that the model was properly sized. Results for 15 kg_f are also obtained.

The maximum von Mises stress experienced in the coating is 8.31 GPa and 8.39 GPa for the 15

and 30 kg_f loading conditions respectively. The maximum von Mises stress experienced in the substrate is 3.10 GPa and 3.23 GPa for the 15 and 30 kg_f loading conditions respectively. All the maximum von Mises stresses occur at the maximum load condition.

Results of Stress Components

The opening stress ($\sigma_{y'y'}$) distribution along the interface is obtained for (15 kg_f) and (30 kg_f). The coating and substrate opening stress distribution match very well as expected due to stress equilibrium perpendicular to the interface [14]. The maximum opening stress occurs near the indentation crater edge after unloading with values of 0.896 GPa (coating) and 0.872 GPa (substrate) for the 15 kg_f loading case and of 1.18 GPa (coating) and 1.16 GPa (substrate) for the 30 kg_f loading case. These simulated opening stresses provide a measure of the coating adhesion strength for the mirror surface and Bullion and Glass Bead laser frosted surface.

To satisfy equilibrium conditions along the coating-substrate interface, the shear stress ($\tau_{x'y'}$) in the coating and substrate materials must be equal and the results agree well with this equilibrium condition [14]. The difference between the coating and substrate shear stress value is minimal except near the indentation crater edge where a nearly 20% difference occurs. The maximum shear stress values along the interface are 1.89 GPa (coating) and 1.67 GPa (substrate) for the 15 kg_f loading case and of 2.16 GPa (coating) and 1.78 GPa (substrate) for the 30 kg_f loading case. These maximum shear stress values occur at maximum loading of the indenter and provide a measure of the coating adhesion strength for the simulated surface types.

The radial stress ($\sigma_{x'x'}$) distributions along the coating-substrate interface for the 15 and 30 kg_f loading cases are obtained. The maximum compressive radial stress occurs at maximum loading, the values for the 15 and 30 kg_f loading conditions are 11.29 GPa and 12.69 GPa. Table 3 summarised the maximum values of these stress components.

5. Conclusions

The stress state at the coating-substrate interface during 15 and 30 kg_f indentation tests has been simulated. Peak stress values were found in the region near the indentation crater edge, which is where failure was observed during experimental testing. Using finite element simulations, the PVD coating deposited on a mirror surface and Glass Bead and Bullion laser frosted surfaces was found to be capable of surviving the loads corresponding to stress values presented in Table 3. The peak opening and shear stresses at the coating-substrate interface provide a characterization of the coating adhesion strength since these two stress components are capable of directly causing delamination growth and coating adhesion failure. Significant compressive radial stress is present in the coating outside the indentation crater. In the presence of coating adhesion defects, this compressive stress can lead to coating buckling and spallation.

The three stress components (opening, shear, and radial compressive) reach their peak near the indentation crater edge, which is the location where coating delamination occurred during experimental testing at higher loads. Now that the stress state at the coating-substrate interface produced during indentation adhesion tests has been simulated and analyzed, a similar process can be performed for the scratch adhesion tests and the results can be compared.

Acknowledgements

The authors gratefully acknowledge the financial supports from the Ontario Centres of Excellence (OCE), Royal Canadian Mint and the Natural Sciences and Engineering Research Council (NSERC) of Canada. Thanks also go to Hibbit, Karlsson and Sorensen, Inc. for making ABAQUS available under an academic licence to Carleton University.

References

[1] Bodor, S., (2010). Personal interview at Royal Canadian Mint, Sept. 28 2010.

[2] Lacombe, R. (2006). Adhesion measurement methods: Theory and Practice. *CRC Press*, pp. 7-73.

[3] Pachler, T., Souza, R. M., Tschiptschin, A. P. (2007). Finite element analysis of peak stresses developed during indentation of ceramic coated steel. *Surface and Coating Technology*, Vol. 202, pp. 1098-1102.

[4] Nygards, C. M., White, K. W., Ravi-Chander, K. (1998). strength of HVOF coating-substrate interfaces. *Thin Solids Films*, Vol. 332, pp. 185-188.

[5] Xu, M., Li, L., Liu, Y., Cai, X., Chen, Q., Chu, P. K. (2007). Experimental tests and numerical simulation studies on nano-indenation of TiN film deposited on N+-implanted aluminum. *Surface and Coatings Technology*, Vol. 201, pp. 6707-6711.

[6] Sun, X., Liu, W. N., Stephens, E., Khaleel, M. A. (2008). Determination of interfacial adhesion strength between oxide scale and substrate for metallic SOFC interconnects. *Journal of Power Sources*, Vol. 176, pp. 167-174.

[7] ABAQUS (2008). ABAQUS Analysis User's Manual. ABAQUS *Online Documentation, Dassault Systèmes*, Version 6.8.

[8] ASTM E18-8b (2008). Standard Test Methods for Rockwell Hardness of Metallic Materials. *ASTM International.*

[9] Bohler Uddeholm (Novembe 15, 2010). Plastic Mold Steel. Retrieved November 15, 2010, from Bohler Uddeholm Web site: http://www.bucorp.com/plastics.htm

[10] Yan, J., Karlsson, A. M., Chen, X. (2007). Determining plastic properties of a material with residual stress by using conical indentation. International Journal of Solids and Structures, Vol. 44, Issue 11-12, pp. 3720-3737.

[11] McLean, D. A. (2010). The characterisation and performance of magnetron sputter coatings on minting dies. Department of Mechanical and Aerospace Engineering, Carleton University. Ottawa, Canada.

[12] Piana, L. A., Pérez, R. E., Souza, R. M., Kunrath, A. O., Strohaecker, T. R. (2005). Numerical and experimental analyses on the indentation of coated systems with different mechanical properties. *Thin Solid Films*, Vol. 491, pp. 197-203.

[13] Benham, P. P., Crawford, R. J., Armstrong, C. G. (1996). Mechanics of Engineering Materials, Prentice Hall, 2nd Ed., pp. 292-521.

[14] Ramalingam, S., Zheng, L. (1995). Film-substrate interface stresses and their roles in the tribological performance of surface coatings. Tribology International, Vol. 28, No. 3, pp. 145-161.

Table1 Material properties of the simulated substrate

Property	**Symbol**	**Value**
Elastic Modulus	E_s	213 GPa
Yield Strength	σ_{ys}	2.35 GPa
Poisson's Ratio	ν_s	0.3
Strain hardening exponent	n_s	15
Yield offset	α_s	0.18

Table 2 Material properties of the simulated coating

Property	**Symbol**	**Value**
Elastic Modulus	E_c	300 GPa
Yield Strength	σ_{yc}	8.2 GPa
Poisson's Ratio	ν_c	0.15
Strain hardening exponent	n_c	100
Yield offset	α_c	1

Table 3 Stress component values for coating adhesion strength characterisation

Stress Component *[material]*	**15 kg_f (Glass Bead)**	**30 kg_f (Mirror and Bullion)**
Maximum Opening stress (GPa) *[average of coating and substrate value]*	0.884	1.17
Maximum Shear stress (GPa) *[average of coating and substrate value]*	1.78	1.97
Maximum Compressive stress (GPa) *[coating value]*	-11.3	-12.7

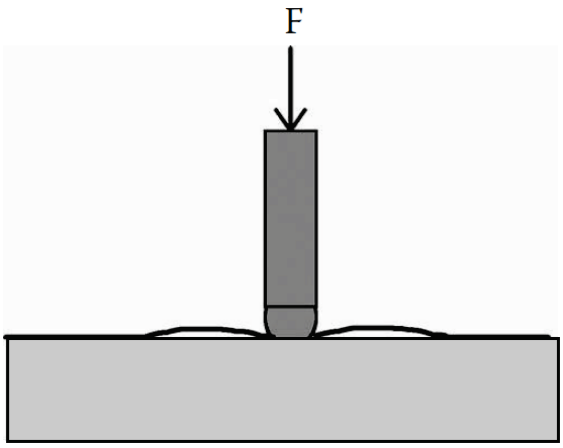

Figure 1. Schematic of indentation test causing coating adhesion failure [2]

Figure 2. Wilson Rockwell 3TT Twin Hardness Tester

Figure 3 Test dies with three-quarter laser frosted surfaces

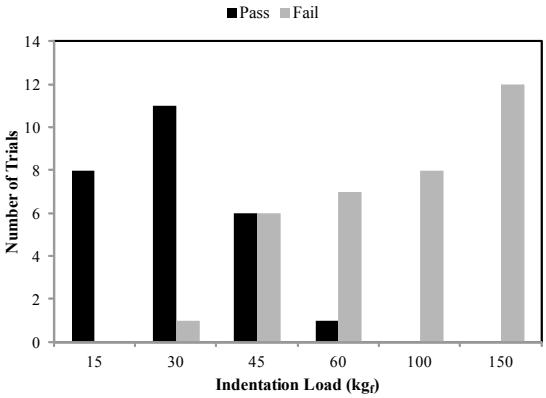

Figure 4 Distribution of the stepped indenation results for the PVD coating on a mirror surface

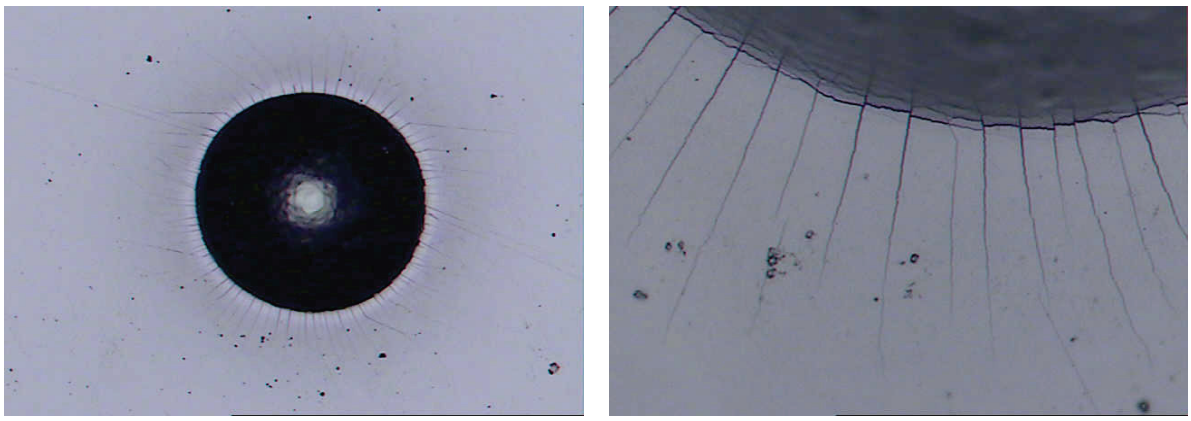

(10X) (50X)

Figure 5 Typical results for the Rockwell-C indentation of the PVD coating on a mirror surface for load 30 kg_f

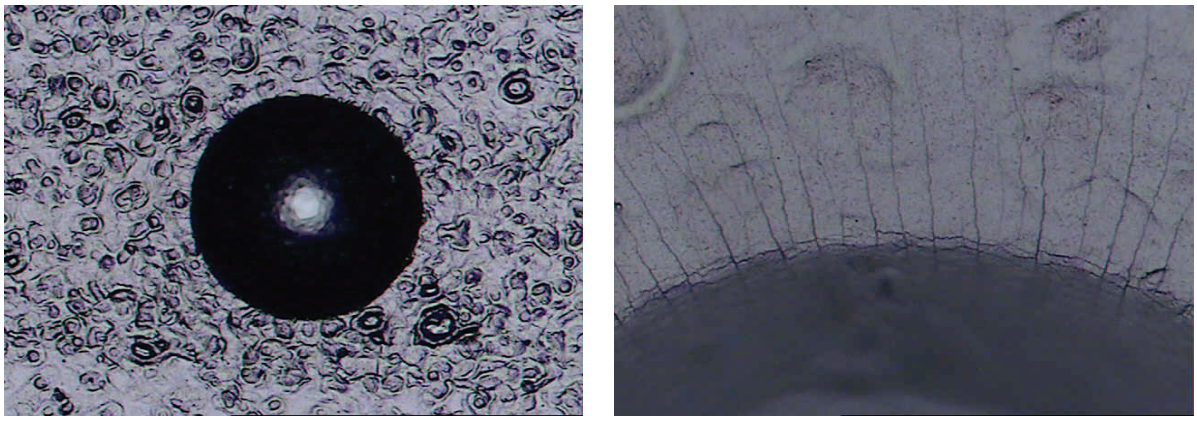

(10X) (50X)

Figure 6 Typical results for Rockwell-C indentation of the PVD coating on a Bullion laser frosted surface for loads of 30 kg_f

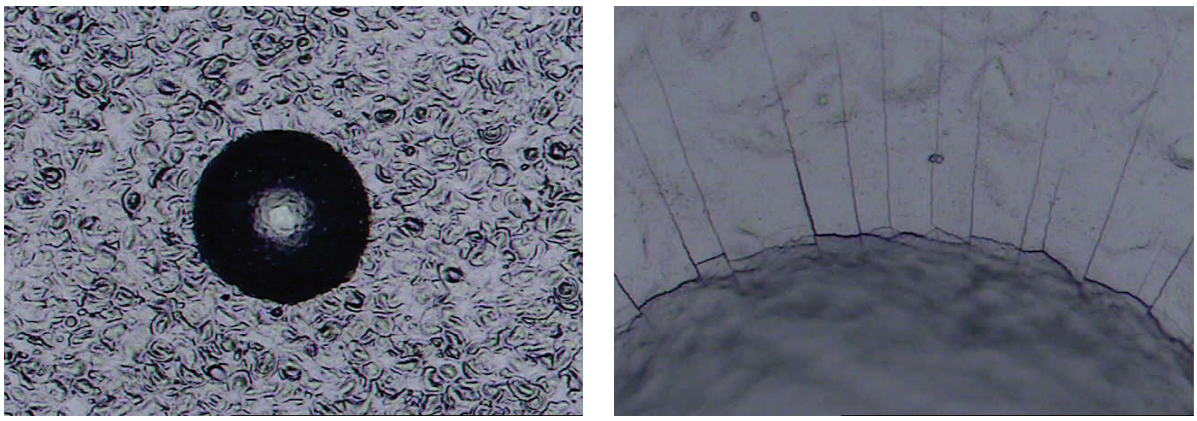

(10X) (50X)

Figure 7 Typical results for Rockwell indentation of the PVD coating on a Glass Bead laser frosted surface for loads of 15 kg_f

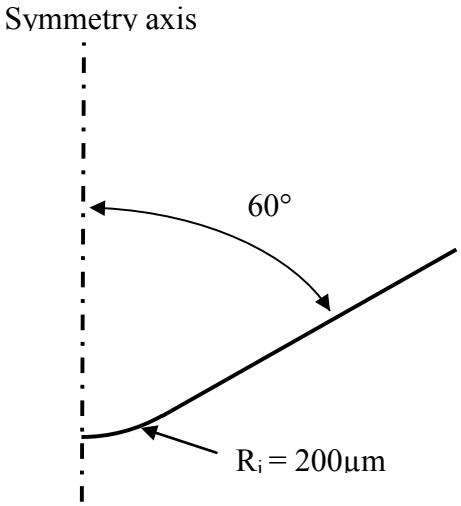

Figure 8 Rockwell C indenter tip geometry

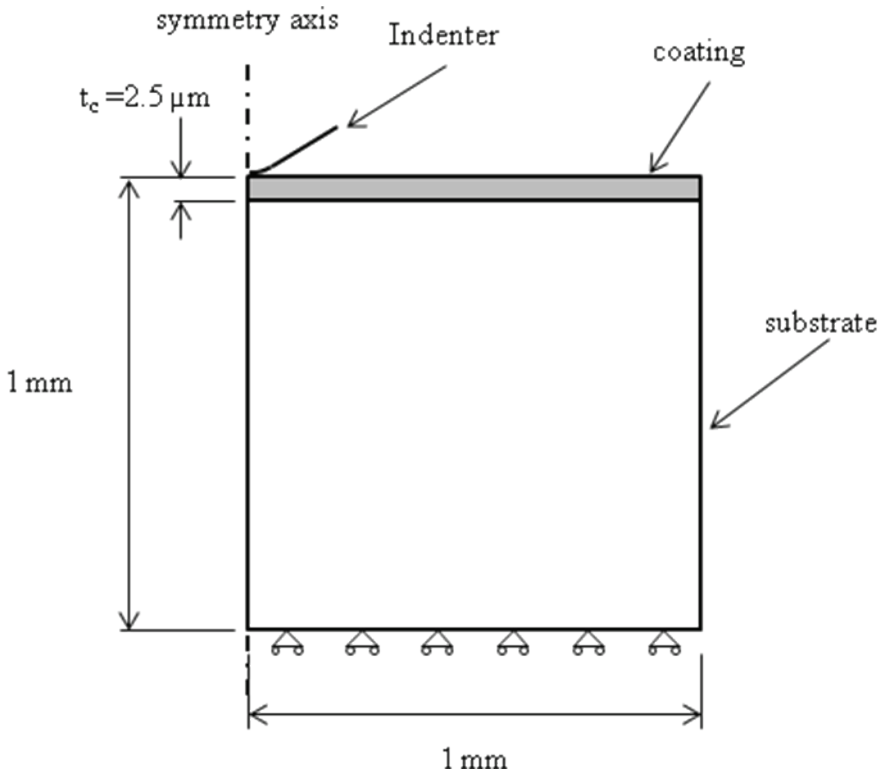

Figure 9 Die geometry and boundary conditions (not to scale)

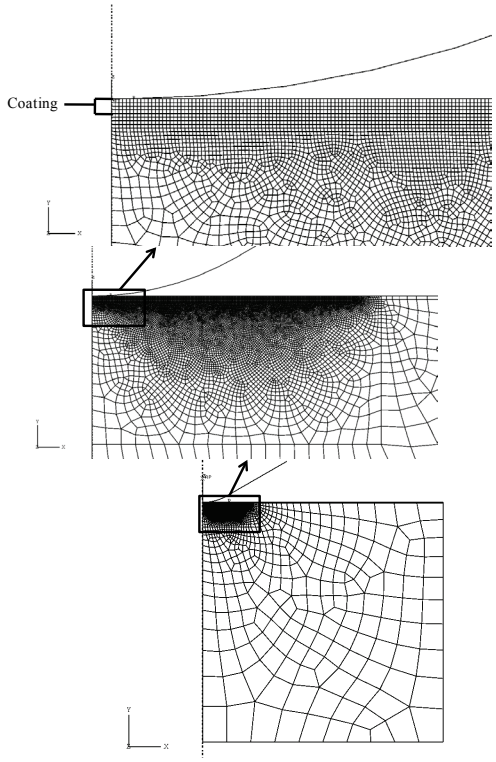

Figure 10 Coating substrate mesh design, 4 element layer coating

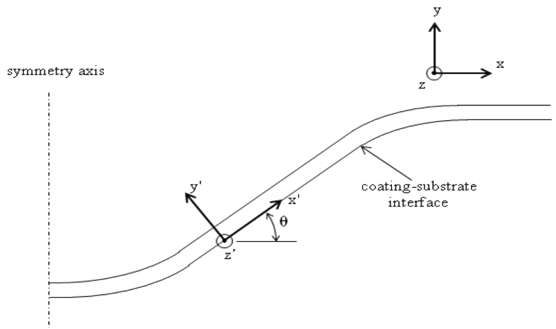

Figure 11 Local coordinate system at the coating-substrate interface

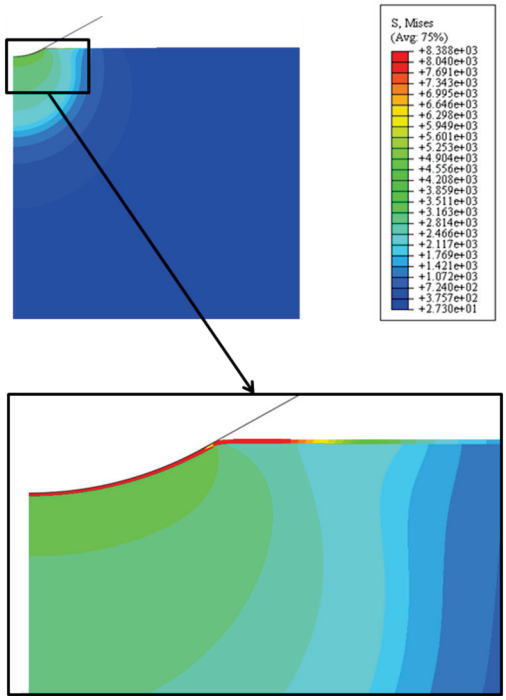

Figure 12 von Mises Stress contour at the 30 kg_f loading condition

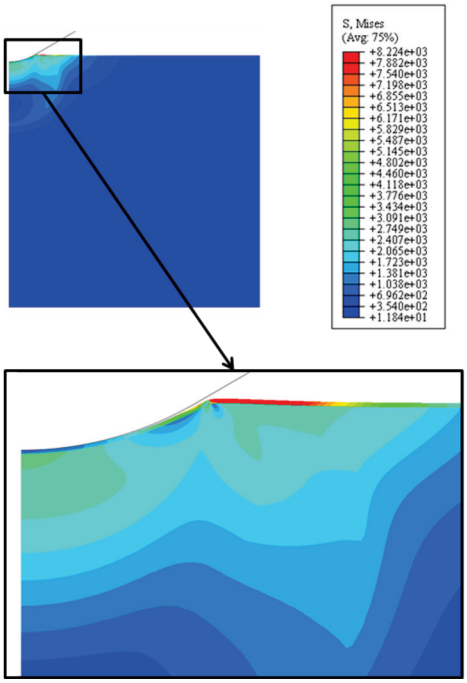

Figure 13 von Mises Stress contour after unloading the 30 kg_f load